Hindawi
Advances in Civil Engineering
Volume 2023, Article ID 7565260, 17 pages
https://doi.org/10.1155/2023/7565260

Research Article

Investigating the Feasibility of Using Concrete Containing Waste Paper Sludge Ash and Pozzolanic Materials to Repair Bridge Stub Columns

F. Delaram,[1] **Y. Mohammadi**,[2] **and M. R. Adlparvar**[3]

[1]*Department of Civil Engineering, Qeshm Branch, Islamic Azad University, Qeshm, Iran*
[2]*Department of Civil Engineering, University of Mohaghegh Ardabili, Ardabil, Iran*
[3]*Department of Civil Engineering, University of Qom, Qom, Iran*

Correspondence should be addressed to Y. Mohammadi; yaghoubm@uma.ac.ir

Received 8 October 2022; Revised 5 January 2023; Accepted 21 January 2023; Published 24 February 2023

Academic Editor: Piotr Smarzewski

In most cases, the bridge columns are underwater, and there is a risk of corrosion. The columns of marine structures and docks also include such problems. In addition to the problem of environmental hazards, the bridge columns may fail due to design problems or increasing needs. The use of waterproof concrete materials as a jacket can have a role in increasing the life of bridges. Studies in recent years show that some waste from paper industries can be used in the construction industry. In the present study, several concrete stub columns were built as bridge columns and retrofitted with concrete jackets containing waste paper sludge ash, silica nanoparticles, aluminium oxide nanoparticles, and acrylic resin. The variables included the geometric shape of the column (square and circular) and the type of nanoparticles used in the jackets (silica and aluminium oxide nanoparticles), and the curing environment of the columns (normal and sulfate environments). The combined use of nanomaterials and waste paper ash is the most important novelty of the present study. The axial loading test was performed on the columns, and the load-deflection diagrams were obtained. The ductility, stiffness, load-bearing capacity, and crack distribution were among the parameters that were used to compare different modes. The proposed jackets increased the carrying capacity by 10 to 38%, depending on the processing curing environment and the type of nanoparticles. The combined use of aluminium oxide nanoparticles and waste paper ash can improve compressive, tensile, and flexural strengths and increase the axial load capacity of bridge columns. The proposed concrete jacket effectively reduces the corrosion of concrete and steel reinforcement and improves the bridge's useful life.

1. Introduction

Over the past few thousand years, bridges have played an important role in developing early civilizations, spreading knowledge, local and global trade, and increasing transportation [1–3]. Therefore, their repair and retrofitting are sensitive and important tasks. In order to improve the seismic performance of infrastructures and increase their carrying capacity, many countries are strengthening and upgrading old bridges [4–6]. All these issues make the engineers do different research in the strengthening field. In most cases, the columns of bridges are underwater, and there is a risk of corrosion. The column of marine structures and docks also include such problems. In addition to the problem of environmental hazards, the column of bridges may fail due to design problems or increasing needs. The use of waterproof concrete materials as a jacket can have a role in increasing the life of bridges.

On the other hand, the porosity of concrete significantly affects water absorption in the concrete structure. The high permeability of concrete allows reactive molecules to enter, which may ultimately lead to the loss of chemical stability of cement products [7–9]. In addition, the low permeability of concrete can improve the resistance to water penetration, sulfate ions, chloride ions, alkali ions, and other harmful substances that cause damage to concrete. The permeability

of concrete has a close relationship with the characteristics of the cement paste pore structure, the number of small cracks in the joint space between the aggregates and the cement paste, and the cracks of the cement paste [10–12]. The pore structure mainly contains interconnected capillary pores that create different pore volumes and sizes. The result of the hydration reaction on cement is a product consisting of a solid body and pores. The pore network of the cement paste provides a matrix for the passage of fluid into the concrete, the development of which depends on a number of factors, including the properties and composition of the concrete constituents, the initial conditions of sealing, and its duration. Temperature, curing time, and humidity are key factors suitable for pore structure [13, 14]. When pozzolanic materials are used as part of cement in concrete, the effectiveness of the initial treatment becomes more important. The driving force for water to enter concrete is not compressive but capillary suction in concrete voids [15]. Therefore, it seems that adding hydrophobic materials to the concrete mix will reduce the water penetration into the concrete due to the reduction of the concrete's tendency to water. Pozzolanic materials can enter these voids and destroy the network connections of the pores. This study investigates the feasibility of hydrophobic concrete and its use in the repair of concrete bridge columns.

Making concrete with recycled materials is one of the topics that have been the focus of the engineering community [16–18]. Waste paper sludge ash and pozzolanic materials were used as a substitute for part of the cement. Ahmad et al. studied the attributes of concrete containing waste paper sludge ash as a partial replacement for cement. They showed that up to 5% of waste paper sludge ash could improve concrete properties [19]. Wong et al. investigated hydrophobic concrete using waste paper sludge ash. They showed that 12% of using waste paper sludge ash could improve the durability attributes of concrete [20]. Fauzi et al. studied the effect of recycled aggregate concrete incorporating waste paper sludge ash as a partial replacement for cement. The findings demonstrated that the waste paper sludge ash and recycled aggregate concrete seem to contribute to the favourable concrete compressive strength [21]. Bui et al. investigated the properties of recycled aggregate concrete containing industrial by-products and waste paper sludge ash. The results showed that waste paper sludge ash considerably improved the mechanical attributes of recycled aggregate concrete at an early age and enhanced the resistance of recycled aggregate concrete to the sulfate environment [22]. Meko and Ighalo investigated concrete's fresh and hardened properties with waste paper sludge ash as cement replacing the material. The Portland cement was partially replaced with 0%, 5%, 10%, 15%, and 20% of waste paper sludge ash. The results showed that the workability of concrete containing waste paper sludge ash decreases as the waste paper ash content increases [23].

The review of studies about waste paper sludge ash [24–29] shows that these materials can be used as a partial replacement for cement. Although waste paper sludge ash can improve the durability properties of concrete, it has little effect on improving the mechanical properties of concrete. Meanwhile, nanoparticles can overcome this weakness and improve the mechanical properties. Therefore, the present study evaluated the combined use of waste paper sludge ash and nanomaterials on the mechanical properties and durability of high-strength concretes.

Due to the almost high percentage of water absorption of this type of concrete, waterproof additives and pozzolanic materials are used to reduce the water absorption. The waste paper sludge ash from paper industries can be used as a raw material in concrete production to repair the column of bridges, which will be evaluated in the present study.

High-performance concrete has been recommended as an advanced engineering material for extremely high strength, ductility, and durability [30]. These features make it possible to use high-performance concrete in the field of increasing resistance. Therefore, concrete jacket to limit and protect bridge columns used in marine environments is of interest [31]. Bridges are sensitive structures because any damage to them causes financial and life losses during and after an earthquake. Due to numerous earthquakes and damage to structures, especially vital arteries, various seismic retrofitting and improvement methods have been increasingly developed in the last few decades. Before carrying out the retrofitting steps, it is very important to study the structure, among which bridges are equally important as strategic and important structures [32–34] (Figure 1).

One of the ways to strengthen the columns of concrete bridges is to use concrete jackets. The advantages of concrete jackets are as follows [32]:

(1) A durable protective jacket that acts as a barrier against the penetration of aggressive elements

(2) Preventing the spalling of the concrete cover of steel reinforcements

(3) The strength of the surface bond between concrete jacket and concrete columns

(4) It can be used in reinforced concrete columns with different shapes due to its excellent performance

Various studies have been done in the field of bridge column strengthening. Li et al. investigated the axial behavior of square-reinforced concrete columns retrofitted with circular steel tubes and concrete jackets. The experimental results showed that reinforced concrete columns' bearing capacity, strength, and ductility increased using the proposed method. The increase in cross-sectional areas and the covering of the column's peripheral surfaces by steel pipes are among the reasons for this increase [31]. Xie et al. investigated the compressive behavior of reinforced concrete columns of bridges with high-strength concrete jackets. This study performed compressive strength tests on 18 reinforced concrete columns with high-strength concrete jackets. The variables were the geometric shape of the base of the columns and the thickness of the jacket. The test results showed that increasing the thickness of the jacket cover for cylindrical columns significantly improves the compressive behavior of the columns, which is less effective in square columns [32]. He et al. investigated the seismic behavior of reinforced concrete columns retrofitted with steel jackets.

Figure 1: Concrete columns with a circular cross section in Guilan province in northern Iran.

Nine reinforced concrete columns were built. The results show that the addition of steel jackets increased the maximum strength of the columns by 1.86–3.44 times [33]. Therefore, in the present study, the feasibility of making waterproof concrete for the repair of bridge columns using waste paper sludge ash and pozzolanic materials was investigated, and its mechanical properties and durability were determined. Different percentages of waste paper sludge ash and synthetic pozzolans were used in producing hydrophobic concrete to repair the column of bridges in the corrosive environment. The most important difference between the current study and other studies is the combined use of nanomaterials and waste paper ash in concrete jackets with the aim of strengthening bridge columns. In fact, in addition to engineering specifications, the main focus of this study is the practical use of this proposed concrete in strengthening bridge columns, which has not been considered in previous studies.

2. Laboratory Program

Laboratory studies were carried out in two different sections. The variables in the first part included the following: (1) the amount of waste paper sludge ash (0, 5, 10, and 15% by weight of cement), (2) the type of nanoparticles (silica and aluminium oxide), (3) the amount of nanoparticles (0 and 2.5% by weight of cement), and (4) acrylic resin (5 and 10% by weight of cement). The results of this section were published in a study conducted by the authors [25] (Table 1). Mechanical properties were evaluated by compressive strength, splitting tensile strength, flexural strength, and ultrasonic pulse velocity tests. Also, the durability of concrete was checked by conducting tests such as water penetration depth, water absorption, and electrical resistivity.

In the second part, a number of concrete columns were built as the columns of the bridge and retrofitted using concrete jackets containing silica nanoparticles, aluminium oxide nanoparticles, waste paper waste ash, and acrylic resin. The variables in this section included the geometric shape of the column (square and circular) and the type of nanoparticles used in the jacket (silica and aluminium oxide), and the curing environment of the columns (normal and sulfated water). The geometric cross section of the base of bridges is generally either circular or square. Therefore, these two common shapes were evaluated in the present study.

On the other hand, bridge foundations are always exposed to corrosion. For this reason, the effect of corrosiveness on the effectiveness of the desired strengthening method was investigated by choosing sulfated environment.

This study uses the most optimal mixing design for retrofitting bridge columns with concrete jackets. After making the examined samples, the best mixing design in terms of mechanical characteristics and durability is the mixed design in which 2.5% of nanoparticles (silica and aluminium), 10% of waste paper sludge ash, and 10% of acrylic resin are used (according to Table 1). Using the mentioned mixing design, a number of reinforced concrete columns representing the bridge columns were selected and subjected to axial loading. In Table 2, the desired columns and variables are presented. Also, in Figure 2, the schematic image of the concrete jacket for bridge columns is presented.

The geometric characteristics of the samples are presented in Figure 3. The diameter and height of the cylindrical samples were considered to be 150 and 450 mm, respectively. Also, the width and height of the cubic samples are 150 and 450 mm, respectively. The effect of changes in the thickness of the proposed jacket was not evaluated in the present study. This thickness was considered equal to 20 mm based on the study of Xie et al. [19].

2.1. Materials. Materials included coarse and fine aggregates, cement, water, superplasticizer, waste paper sludge ash, silica nanoparticles, aluminium oxide nanoparticles, and acrylic resin. The gravel used in this project was of crushed type. The density of sand was 2600 kg/m^3, and the specific weight of gravel was 2650 kg/m^3. The grading of sand and gravel is in accordance with the ASTM C330 [35].

Type II Portland cement was used as the main adhesive material according to ASTM C150 [36]. The density of cement was 1.95 g/cm^3.

Silica nanoparticles are an artificial material consisting of very fine SiO_2 particles, which, like cement, have high pozzolanic properties. The powder of this material is 99.9% silica, and the density is 0.2 g/cm^3. The specific surface area of silica nanoparticles is 50 to 100 m^2/g. The diameter of particles is about 50 to 100 nm. The specifications of silica nanoparticles are presented in Table 3.

Aluminium oxide nanoparticles are white synthetic material that consists of very small particles of Al_2O_3. This material is used to improve the properties of ceramics and solve their brittleness problem, increasing the erosion resistance of coatings and heat resistance [37]. Alumina in the nanoaluminium powder used in this research is more than 99%, its density is 3.89 g/cm^3, and the specific surface area of these nanoparticles is more than 138 m^2/g. The diameter of its solid particles is about 20 nm. The characteristics of aluminium oxide nanoparticles are presented in Table 3.

Table 1: The properties of specimens containing waste paper sludge ash, silica nanoparticle, aluminium oxide nanoparticles, and acrylic resin [25].

Mix ID	Slump (mm)	Compressive strength (MPa) Days			Splitting tensile strength (MPa)	Flexural strength (MPa)	Ultrasonic pulse velocity (UPV)	Water absorption (%)	Water penetration depth (mm)	Electrical resistivity (kΩ-cm)
		7	28	90						
P0	46	38.9	57.1	79.6	3.91	4.60	3.79	5.10	5.31	89.00
P0S	47	46.3	66.1	91.3	4.49	5.10	3.87	3.98	4.41	105.00
P0AL	56	44.6	65.3	89.2	4.21	4.93	3.89	4.08	4.14	105.00
P5	51	39.1	58.9	77.6	3.93	4.65	3.84	4.13	3.98	98.00
P5S	54	47.6	67.2	88.9	4.48	5.23	3.88	3.77	4.25	109.00
P5AL	65	46.3	66.5	87.3	4.32	5.11	4.04	3.83	4.11	108.00
P10	68	40.3	60.3	79.13	3.86	4.69	4.09	3.93	3.91	106.00
P10S	73	49.3	72.1	97.3	4.52	5.26	3.91	3.62	3.71	118.00
P10AL	78	48.7	70.2	96.4	4.27	5.19	3.81	3.67	4.26	117.00
P15	76	37.1	55.6	75.3	3.82	4.53	4.03	3.72	4.15	115.00
P15S	79	46.3	65.7	90.3	4.41	5.22	4.06	3.32	3.95	149.00
P15AL	81	45.2	65.5	89.3	4.18	5.12	3.89	3.37	3.76	147.00
P10-AC5	692	39.3	59.3	78.2	3.46	4.49	4.02	3.56	3.62	120.80
P10S-AC5	684	44.8	70.6	97	4.18	5.03	4.17	3.20	3.58	135.70
P10AL-AC5	665	43.9	68.3	95.9	4.01	4.93	4.18	3.24	3.5	133.10
P10-AC10	642	38.6	59	77.1	3.21	4.42	4.37	3.35	3.46	129.60
P10S-AC10	614	43.5	67.3	96.3	3.88	4.92	4.21	3.11	3.38	144.30
P10AL-AC10	609	41.9	66.3	94.3	3.69	4.78	4.35	3.12	3.36	141.10

Note. P: waste paper sludge ash, S: silica nanoparticle, AL: aluminium oxide nanoparticles, and AC: acrylic resin.

Table 2: The desired columns and variables.

No	Column name	The type of nanoparticles used in the jacket	The amount of waste paper sludge ash used in the jacket	Environmental conditions	The geometric shape of the column
1	Ci-NE	—	—	Normal	Circular
2	Ci-NE-Ns	Silica nanoparticles	10	Normal	Circular
3	Ci-NE-Al	Aluminium nanoparticles	10	Normal	Circular
4	Ci-SE	—	—	Sulfate	Circular
5	Ci-SE-Ns	Silica nanoparticles	10	Sulfate	Circular
6	Ci-SE-Al	Aluminium nanoparticles	10	Sulfate	Circular
7	Sq-NE	—	—	Normal	Square
8	Sq-NE-Ns	Silica nanoparticles	10	Normal	Square
9	Sq-NE-Al	Aluminium nanoparticles	10	Normal	Square
10	Sq-SE	—	—	Sulfate	Square
11	Sq-SE-Ns	Silica nanoparticles	10	Sulfate	Square
12	Ci-SE-Al	Aluminium nanoparticles	10	Sulfate	Square

Ci: column with circular cross section, Sq: column with square cross section, NE: normal water environment, SE: sulfate water environment, Ns: silica nanoparticles, and Al: aluminium nanoparticles.

This research investigates the effect of adding waste paper sludge ash to the production of high-strength concrete. Waste paper sludge ash obtained from the Iran wood and paper factory (Chuka). This company has accumulated a lot of waste from the paper production process in recent decades, and its ash can be used to produce concrete. The waste from the factory was kept in the open air for seven days and then burned at a temperature of 700 degrees Celsius. Chemical compounds and mineral oxides in recycled sludge ash were evaluated using X-ray fluorescence spectroscopy (XRF) (Table 3). Iran's wood and paper mill sludge was a solid waste consisting of fiber residues and ash produced from the paper and pulping process. They were prepared and used as a part of cement in this research to evaluate its

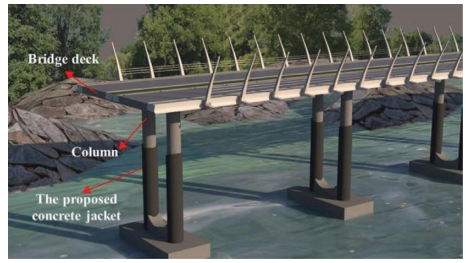

Figure 2: A schematic picture of the place where the concrete jacket is used for bridge columns.

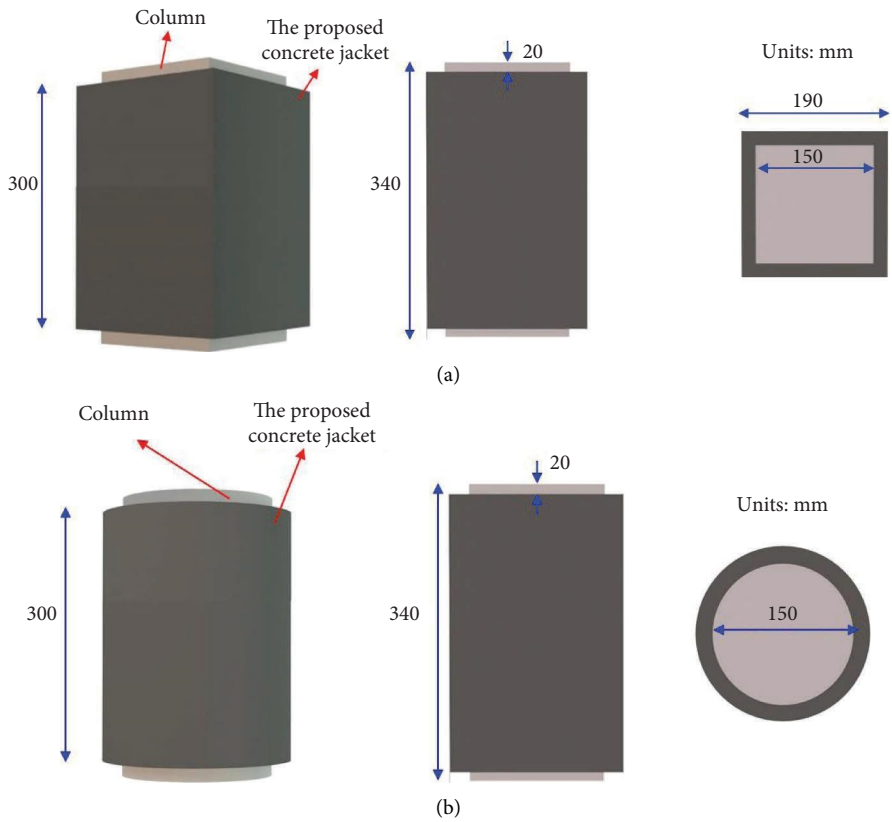

Figure 3: Geometric characteristics of the studied columns: (a) square section and (b) circular section.

Table 3: Chemical characteristics of the binder materials.

Components	Cement	AlNPs	SNPs	WPSA
Al_2O_3	4.95%	99≥%	—	6.83
CaO	62.95%	≤25 ppm	—	25.43
SiO_2	21.27%	—	≥99.98%	10.79
Fe_2O_3	4.03%	≤80 ppm	—	0.46
MgO	1.55%	—	—	0.87
SiO_3	2.26%	—	—	0.32
K_2O	0.65%	—	—	0.22
Na_2O	0.49%	≤70 ppm	—	0.15
MnO_2	—	≤3 ppm	—	—
Cr	—	≤4 ppm	—	—
Co	—	≤2 ppm	—	—
LOI	—	—	≤1.00	54.34
Specific gravity (g/cm^3)	0.75	3.89	0.5	2.81
Specific surface area (m^2/g)	326	138	200	168

potential for concrete production based on the concept of biological refining.

The brand name of the used superplasticizer is Zhikava, and its specifications are presented in Table 4. This product is made according to ASTM C494 [38], its color is brown, and its state is liquid. Also, the specific weight of this superplasticizer is 1.1 g/cm^3.

The water used in making concrete should be clean and smooth. Avoid using water containing a large amount of any substance that can damage concrete and reinforcement, such as oils, alkalis, salts, and organic substances. Potable water is generally considered satisfactory for making concrete [39]. Potable water was used to make concrete samples [40].

Acrylic resin solid powder has been used in a number of concrete samples in the amount of 5 and 10 percent by weight of cement. According to the manual, this product is recommended for producing all kinds of construction

Table 4: Some properties of acrylic resin used.

pH	9-10
MMFT (°C)	>20
Tg (°C)	+25
(±%1) solid percentage	50
Density (g/cm^3)	1.05
Viscosity (cP)	400–700

materials and colors for interior and exterior use, fabric finishing, and adhesion to cement, asbestos, and concrete. This resin is often used as a primer in silicate and multicolor paints. This resin is prepared from the family of copolymer emulsion resins based on styrene-acrylic and has excellent adhesion and high resistance to water. This resin is a strong binder in producing interior and exterior water-based paints for use on wood. It has a very high resistance to washing and atmospheric factors. Emulsion styrene acrylic resin (water-based) is produced from the polymerization of acrylic acid and methacrylic acid monomers and their derivatives and styrene monomer. Emulsion styrene acrylic resin (water-based) has good tensile strength and resistance to ultraviolet light. Acrylic resins are generally divided into two main groups: thermoplastic and thermoset. These polymers are usually available in the market in two forms, emulsion and water-soluble powder. These materials are known as carbomers in the commercial term. Carbomer is a term used for a series of primary polymers made from acrylic acid. Its solid type is in the form of white powder. Resin is the first layer of protective coatings in the repair discussion. Often, this resin layer is applied to the surface by applying one hand, and the product thickness is about 100 to 300 microns. The important point in using different types of resin bases is the appropriate time of applying the resin and its thickness, which should be considered in the discussions related to restoration. Table 4 presents some characteristics of the acrylic resin used.

Acrylic resins are antimoss, algae, and bacteria and do not allow the growth and accumulation of these materials on the surface. This resin is highly resistant to detergents, radiation, and CO_2 gas. This material is used in two ways without mixing it with cement and other materials and in cement mortars and grouts. This material is often used as a final layer. Among other uses, it is an additive with cement that is added to concrete and improves cement properties, including cement adhesion, preventing water loss, increasing the durability and stability of concrete, and reducing permeability.

2.2. Experimental Test. The effect of concrete jackets containing waste paper sludge ash, silica nanoparticles, and aluminium oxide nanoparticles on the resistance of bridge columns was investigated. For this purpose, an axial loading test was performed in normal water and sulfated environments.

Polycab pipe was used to make cylindrical concrete samples. All samples' mechanical and geometric characteristics were considered the same in the state without retrofitting. For the construction of the concrete jacket, a larger diameter polycab pipe was used to ensure the jacket's thickness, equal to 20 mm, on each side. The jacket materials included 2.5% nanoparticles (silica and aluminium), 10% waste paper sludge ash, and 10% acrylic resin (P10AL-AC10 and P10S-AC10). A distance of 10 mm was considered between the concrete columns and the cladding at both ends of the samples. Figure 4 presents some of the samples and their manufacturing steps.

A loading frame and hydraulic jack with a capacity of 200 tons were used to apply compressive axial load. This jack has the ability to record deflection up to 50 mm. How to place the samples on the frame and the details of the loading device are shown in Figure 5. The load was applied by a hydraulic jack vertically and along the longitudinal axis of the member, and the deflection corresponding to it until the moment of final failure was recorded by the deflection meter of the device. The deflection meter is connected to the hydraulic jack.

2.3. Mixture Design. In this study, the ACI 211 [41] mixing design method, which is one of the most effective methods available, has been used. In Table 5, the mixture design of samples containing waste paper sludge ash, nanoparticles, and the mixing plan of samples containing waste paper sludge ash, nanoparticles, and acrylic resin are presented. The concrete jacket strength class was chosen to achieve concrete with a 28-day compressive strength between 50 and 60 MPa. Table 5 also shows the mixing plan of the columns in the state without retrofitting.

3. The Results of Strengthening the Columns Using the Proposed Jacket

3.1. Load-Deflection Curves. The results of strengthening concrete columns that were built to represent bridge columns have been presented in this part. As mentioned, after the construction of the examined samples, the best mixing design in terms of structure, mechanical characteristics, and durability is the design in which 2.5% of nanoparticles (silica and aluminium), 10% of waste paper sludge ash, and 10% acrylic resin were used. A number of reinforced concrete columns representing the bridge column were selected and subjected to axial loading.

The variables include the geometrical shape of the column (circular and square), the column curing environment (normal and sulfated), and the type of nanoparticles used in the jacket (silica nanoparticles and aluminium oxide nanoparticles).

Axial load-deflection curves were used to investigate the behavior of columns in different states. Figure 6 shows a schematic picture of load-deflection behavior and desired parameters. This diagram presents the axial reaction forces against the axial shortening of reinforced columns with the proposed jacket. In general, three behavior modes can be observed in the graphs: the elastic phase, the nonlinear phase, and the failure phase (Recession). In the elastic stage (i.e., ab curve), the sample's compressive strength increases almost linearly with the deflection. After the first stage, in the

Figure 4: Pictures of the manufacturing stages of cylindrical samples.

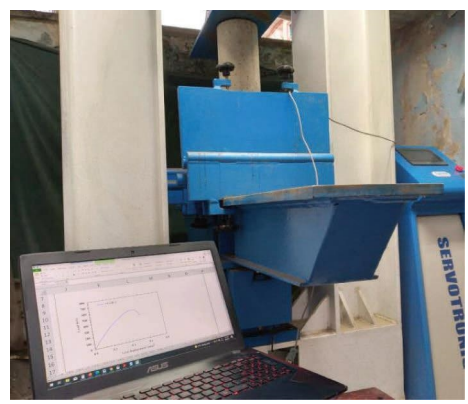

Figure 5: The loading jack used for the axial compressive strength test of the columns.

Table 5: Mixture design (kg/m^3).

Mix code	Cement	Waste paper sludge ash	Silica nanoparticles	Aluminium oxide nanoparticles	Acrylic	Sand	Gravel	Superplasticizer
P0	550	0	0	0	0	705	1075	3.85
P0S	536.25	0	13.75	0	0	705	1075	3.98
P0AL	536.25	0	0	13.75	0	705	1075	4.10
P5	522.5	27.5	0	0	0	705	1075	4.85
P5S	508.75	27.5	13.75	0	0	705	1075	5.10
P5AL	508.75	27.5	0	13.75	0	705	1075	5.21
P10	495	55	0	0	0	705	1075	5.36
P10S	481.25	55	13.75	0	0	705	1075	5.46
P10AL	481.25	55	0	13.75	0	705	1075	589
P15	467.5	82.5	0	0	0	705	1075	6.21
P15S	453.75	82.5	13.75	0	0	705	1075	6.43
P15AL	453.75	82.5	0	13.75	0	705	1075	6.81
P10-AC5	467.5	55	0	0	27.5	705	1075	5.48
P10S-AC5	453.75	55	13.75	0	27.5	705	1075	5.53
P10AL-AC5	453.75	55	0	13.75	27.5	705	1075	5.64
P10-AC10*	440	55	0	0	55	705	1075	5.71
P10S-AC10*	426.25	55	13.75	0	55	705	1075	5.89
P10AL-AC10*	426.25	55	0	13.75	55	705	1075	5.93
Columns in the state without retrofitting	250	0	0	0	0	705	1075	0

*The optimum mixed design used in the concrete jacket.

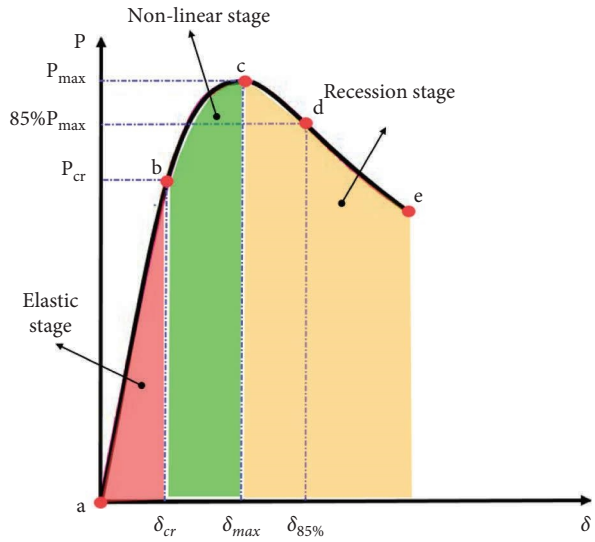

Figure 6: The overall load-deflection behavior of the columns investigated in the current study.

second stage (i.e., curve ab in Figure 6), the samples start to perform nonlinearly due to the cracking of the proposed concrete covers and the nonlinear compressive behavior of the central concrete column. At the end of the nonlinear stage, all samples reach their ultimate resistance (i.e., point b in Figure 6). In the failure stage (i.e., the ce curve in Figure 6), the samples' compressive strength decreases rapidly with the applied deflection load.

According to the considered variables, two columns were made for each state, and the average of the specified parameters in Figure 7 was reported as the final number. In the following, the load-deflection diagrams and images related to the failure of the samples are presented, and then, the effect of each variable parameter is evaluated separately.

The Ci-NE column is a column that was made as a control sample, and its cross section was considered circular and kept in a normal water environment. Figure 7(a) shows the axial load-deflection diagram of this column. The average crack load and deflection were 257.5 kN and 0.15 mm, respectively. Also, this column's average maximum load and deflection were 543.5 kN and 0.455 mm.

The Ci-NE-Ns column is a column retrofitted by a concrete jacket containing 2.5% silica nanoparticles and 10% waste paper sludge ash and kept in a normal water environment. According to the axial load-deflection diagram in Figure 7(b), the maximum load and the corresponding deflection were equal to 752 kN and 0.54 mm, respectively. On the other hand, the crack load was 407 kN, and the crack deflection was 0.15 mm. The addition of the proposed jacket caused the maximum load of the column to increase by about 38% compared to the control sample. The compression areas of the columns can be strengthened at the base of the bridges by using the proposed jacket. By enclosing the central core of concrete, the used concrete jacket improved the transferring force between the old and new materials and could improve the bearing capacity of the column.

The Ci-NE-Al column is a column retrofitted by a concrete jacket containing 2.5% aluminium oxide nanoparticles and 10% waste paper sludge ash and kept in a normal water environment. According to the axial load-deflection diagram in Figure 7(c), the maximum load and the corresponding deflection were equal to 732.5 kN and 0.53 mm, respectively. The crack load was 367 kN, and the crack deflection was 0.53 mm. The addition of concrete jackets in which the combination of aluminium oxide nanoparticles and waste paper sludge increased the bearing capacity of the columns kept in a normal water environment by about 35% compared to the corresponding control sample.

The positive effect of using aluminium oxide nanoparticles in improving the strength of the bridge column confirms the results of other studies in the field of improving the mechanical characteristics of concrete [42–45]. Based on previous research, aluminium oxide nanoparticles can react with calcium hydroxide resulting from cement hydration and lead to calcium silicate gel, which is an essential factor in concrete strength. In this study, the combined use of aluminium oxide nanoparticles and waste paper sludge ash was also effective, and its use in the concrete jacket strengthened the column.

In the diagram of Figure 7(d), the axial load-deflection curve of the Ci-SE column is presented. This column was used as a control sample and was kept in a sulfated environment. Crack load and maximum load of the Ci-SE column were obtained as 328.5 and 530.5 kN, respectively.

Also, deflections corresponding to crack and maximum loads were obtained as 0.195 and 0.545 mm, respectively. The sulfated water environment has caused the bearing capacity of the column to decrease by about 3%. In the following, the results related to strengthening this column using two different proposed concrete jackets are presented.

The Ci-NE-Ns column is a column retrofitted by a concrete jacket containing 2.5% silica nanoparticles and 10% waste paper sludge ash and kept in a sulfated water environment. According to the axial load-deflection diagram in Figure 7(e), the maximum load and the corresponding deflection were equal to 706 kN and 0.545 mm, respectively. On the other hand, the crack load was equal to 330.5 kN, and the crack deflection was equal to 0.195 mm. The addition of the suggested jacket caused the maximum load of the column to increase by about 33%.

The Ci-SE-Al column is a column retrofitted by a concrete jacket containing 2.5% aluminium oxide nanoparticles and 10% waste paper sludge ash and kept in a sulfated water environment. According to the axial load-deflection diagram in Figure 7(f), the maximum load and the corresponding deflection were equal to 708.5 kN and 0.52 mm, respectively. On the other hand, the crack load was 333 kN, and the crack deflection was 0.21 mm.

After presenting the results related to the circular samples, the results related to the square columns will be presented to investigate the effect of the geometric shape on the results. The sq-NE column was used as a control sample, and its cross section was considered square and kept in a normal water environment. Figure 7(g) shows the axial

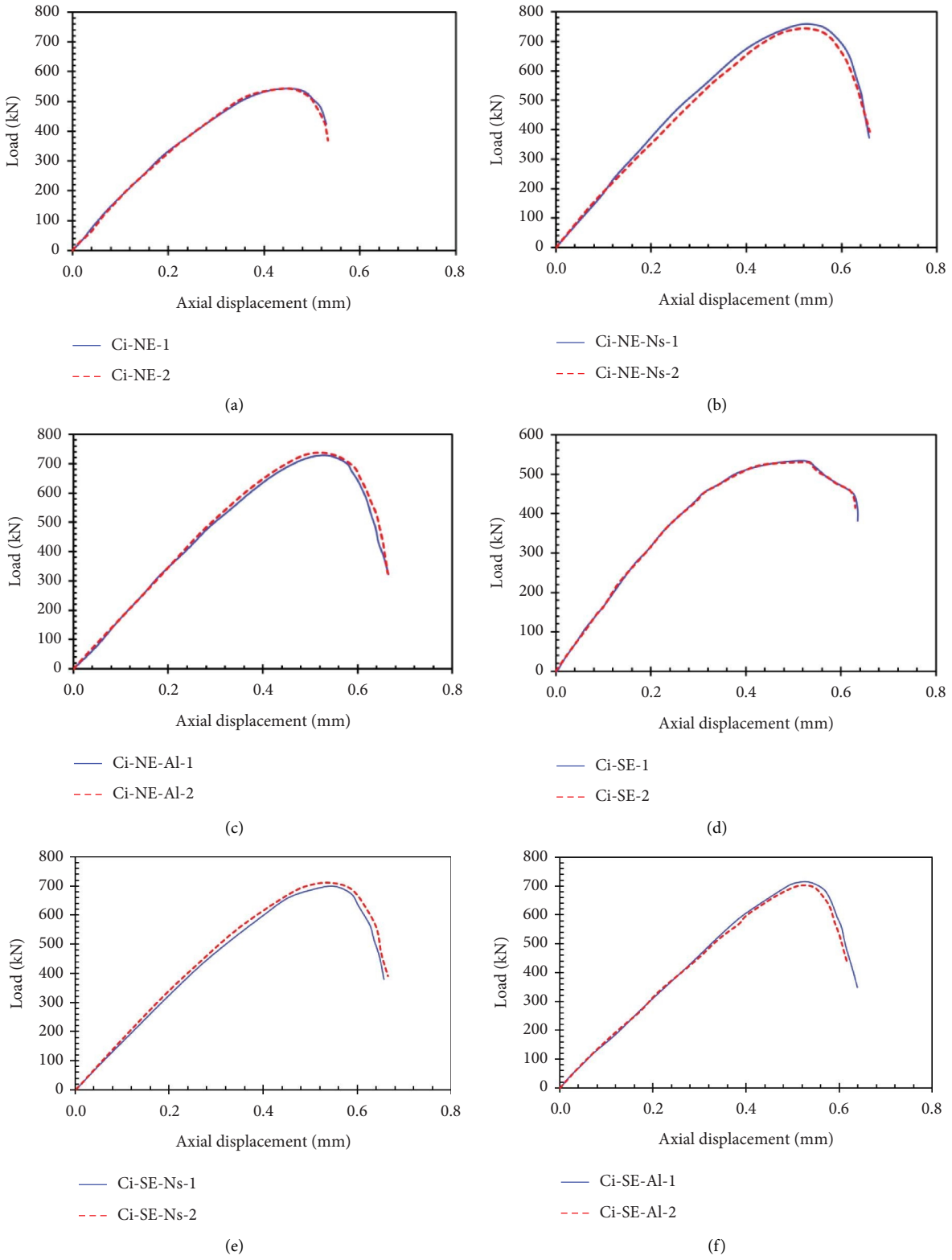

Figure 7: Continued.

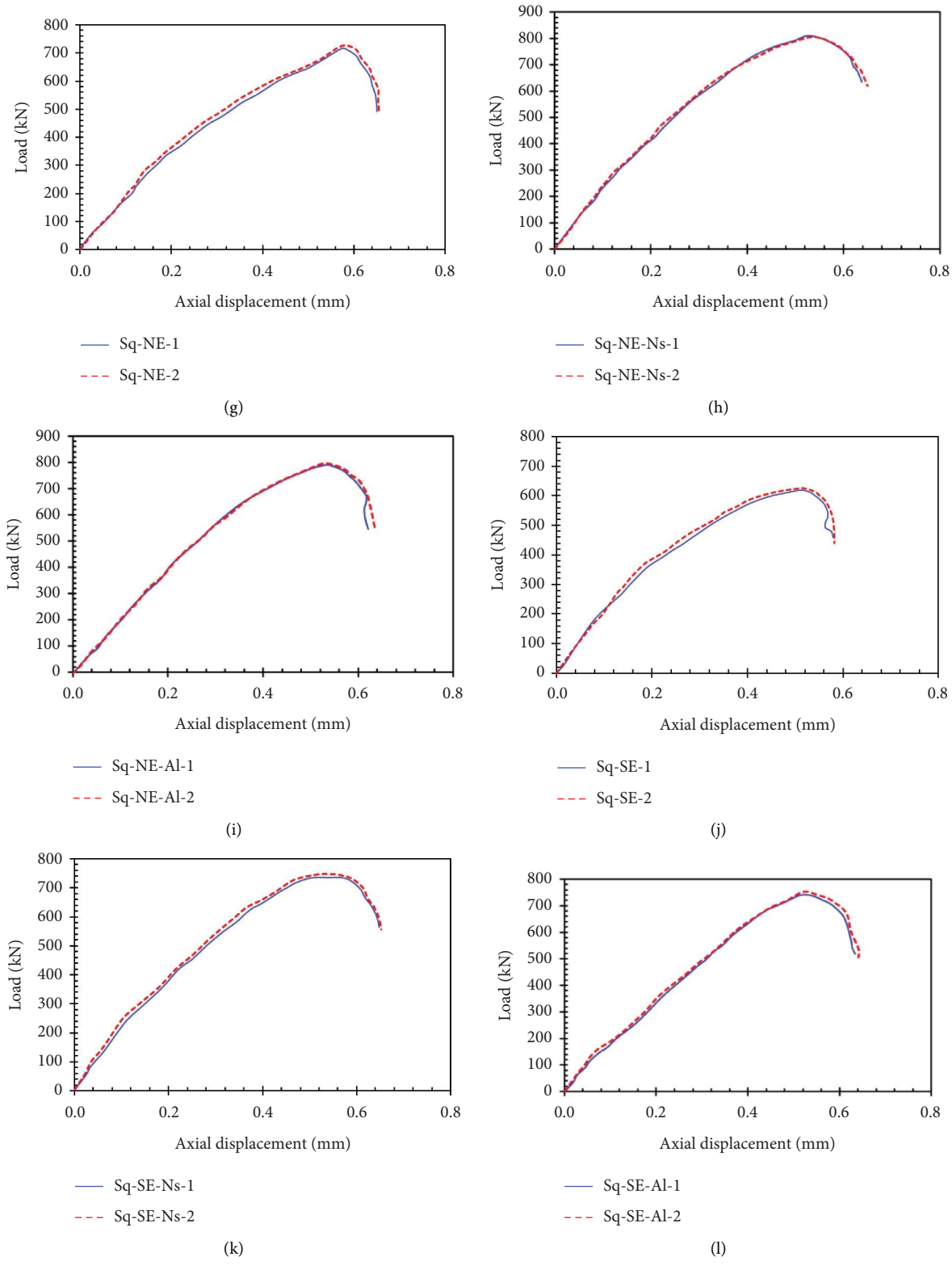

Figure 7: The load-deflection curves of the columns: (a) Ci-NE, (b) Ci-NE-Ns, (c) Ci-NE-Al, (d) Ci-SE, (e) Ci-SE-Ns, (f) Ci-SE-Al, (g) Sq-NE, (h) Sq-NE-Ns, (i) Sq-NE-Al, (j) Sq-SE, (k) Sq-SE-Ns, and (l) Sq-SE-Al.

load-deflection diagram of this column. The crack load and crack deflection were equal to 342 kN and 0.185 mm, respectively. This column's maximum load and deflection were equal to 719.5 kN and 0.57 mm.

The Sq-NE-Ns column is a column retrofitted by a concrete jacket containing 2.5% silica nanoparticles and 10% waste paper sludge ash and kept in a normal water environment. According to the axial load-deflection diagram in Figure 7(h), the maximum load and the corresponding deflection were equal to 805 kN and 150 mm, respectively. On the other hand, the crack load and crack deflections were 560 kN and 0.52 mm. The addition of the suggested jacket has caused the maximum load of the column to increase by about 12%.

The Sq-NE-Al column is retrofitted by a concrete jacket containing 2.5% aluminium oxide nanoparticles and 10% waste paper sludge ash and kept in a normal water environment. According to the axial load-deflection diagram in Figure 7(i), the maximum load and the corresponding deflection were equal to 792.5 kN and 0.525 mm, respectively. On the other hand, the crack load and crack deflection of the column were 456.5 kN and 0.235 mm.

The diagram of Figure 7(j) shows the axial load-deflection curve of the Sq-SE column. This column was used as a control sample and was kept in a sulfated environment. The crack and maximum loads of the Sq-SE column were obtained as 336 and 622 kN, respectively. Also, deflections corresponding to crack and maximum loads were obtained as 0.175 and 0.52 mm, respectively.

The Sq-NE-Ns column is a column retrofitted by a concrete jacket containing 2.5% silica nanoparticles and 10% waste paper sludge ash and kept in a sulfated water environment. According to the axial load-deflection diagram in Figure 7(k), the maximum load and the corresponding deflection were equal to 744.5 kN and 0.54 mm, respectively. Also, the crack load was equal to 441.5 kN, and the crack deflection was equal to 0.225 mm. The addition of the suggested jacket has caused the maximum load of the column to increase by about 20%.

The Sq-SE-Al column is retrofitted by a concrete jacket containing 2.5% aluminium oxide nanoparticles and 10% waste paper sludge ash and kept in a sulfated water environment. According to the axial load-deflection diagram in Figure 7(l), the maximum load and the corresponding deflection were equal to 747 kN and 0.525 mm, respectively. On the other hand, the crack load of the column was equal to 372.5 kN, and the crack deflection was equal to 0.22 mm. The combined use of aluminium oxide nanoparticles and waste paper sludge ash has caused, and in addition to improving the durability of concrete, its compressive, tensile, and flexural strengths have also increased, thus increasing the axial load capacity of bridge columns. The proposed concrete jacket can effectively reduce the corrosion of concrete and reinforcements used and increase the bridge's useful life.

Table 6 provides a summary of some of the outputs resulting from the axial loading of the columns.

3.2. Failure Modes. In Figure 8, the failure modes of the column specimens are presented. The cracks created on the peripheral surfaces of the columns were marked using bold lines. According to the cracks created on the peripheral surfaces of the control samples, it can be stated that the concrete jackets containing nanoparticles and waste paper sludge ash by creating external confinement in the critical areas or the entire exterior surface increased ductility (the ductility values are presented in Table 6) and cause the columns to withstand more forces. The pozzolans used in the proposed concrete jackets improved the load-bearing capacity by improving the durability properties and physical structure of concrete. The use of waste paper sludge ash in combination with silica nanoparticles and aluminium oxide nanoparticles was used to improve the porosity of concrete. By reducing the large capillary pores, they improved the concrete structure and reduced the distribution of cracks in the columns.

By examining the failure modes of the column specimens, it can be seen that there is no significant separation between the concrete jacket and the concrete surface of the main column. The issue of adhesion of concrete jackets to the surface of old concrete is very important; if there is no continuity, the jacket is not very effective in bearing the load. But if the necessary adhesion is created, the load will increase, and the necessary continuity will be provided. Nanosilica and aluminium oxide nanoparticles, by a high specific surface, are combined with hydrated cement and act very well in terms of adhesion, preventing the production of more calcium hydroxide crystals and filling fine cracks.

On the other hand, the corrosion of steel reinforcement in concrete and sulfate invasion is considered to be the most important factors of damage to concrete structures [46–48]. Especially in marine areas, due to the presence of destructive elements such as chlorides and sulfates, this type of damage is observed more often. Also, climatic conditions such as high heat and humidity increase the destruction of structures because temperature intensifies chemical reactions, and humidity is necessary to carry out destruction reactions. Therefore, the performance of the proposed concrete jacket in strengthening the bridge column in the sulfated environment was also evaluated in the present study. As can be seen in columns with a circular cross section, the change in the storage environment has a greater effect on the number and distribution of cracks formed. The number and length of the cracks created in the circular columns placed in the environment of sulfated water are many times more than the cracks created in the circular columns placed in the normal water environment.

3.3. Comparison of the Maximum Load of Columns in Different Modes. In the previous sections, the efficiency of the proposed concrete jacket was evaluated from the qualitative and visual aspects. In the following, the effectiveness of this jacket has been investigated from a quantitative aspect, and to what extent the proposed coating affects the bearing

Table 6: The results of strengthening the columns.

No	Column name	Initial stiffness (N/mm)	Maximum load (kN)	Ductility
1	Ci-NE	1.75	543.5	1.1
2	Ci-NE-Ns	1.88	752	1.14
3	Ci-NE-Al	1.83	732	1.14
4	Ci-SE	1.33	530.5	1.08
5	Ci-SE-Ns	1.77	706	1.13
6	Ci-SE-Al	1.52	708.5	1.14
7	Sq-NE	1.80	719	1.08
8	Sq-NE-Ns	2.26	805	1.19
9	Sq-NE-Al	1.98	792.5	1.16
10	Sq-SE	1.75	622	1.06
11	Sq-SE-Ns	1.97	744.5	1.17
12	Ci-SE-Al	1.77	747	1.16

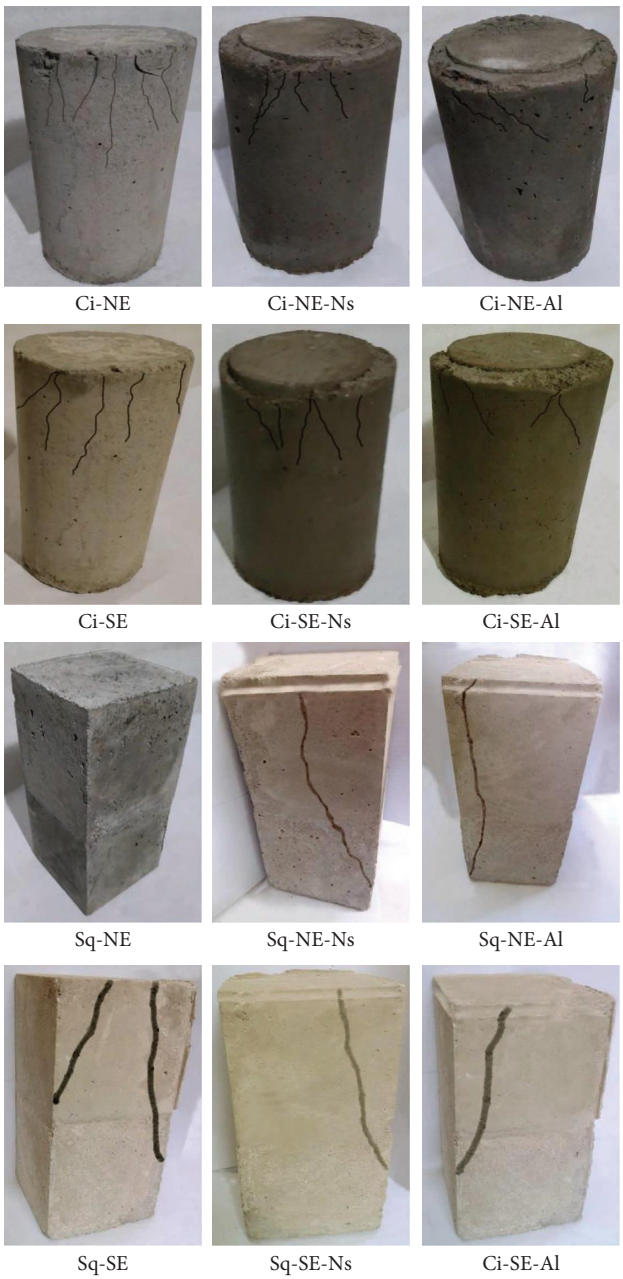

Figure 8: Failure modes.

capacity, formability, and stiffness is evaluated. In Figure 9, the maximum load of the samples in different modes is compared with each other. The use of the proposed jacket in all cases increased the carrying capacity from 10 to 38% depending on the curing environment and the type of nanoparticles (Figure 9). The bearing capacity of Ci-NE, Ci-NE-Ns, and Ci-NE-Al columns is 543.5, 752, and 732.5 kN, respectively. The use of concrete jacket containing silica nanoparticles, waste paper sludge ash, and acrylic resin in the samples cured in a normal water environment increased the bearing capacity by 38% and 34.8%, respectively.

The bearing capacity of Ci-SE, Ci-SE-Ns, and Ci-SE-Al columns is 530.5, 706, and 708.5 kN, respectively. The use of concrete jackets containing silica nanoparticles, waste paper sludge ash, and acrylic resin in cylindrical samples cured in a sulfated water environment increased the bearing capacity by 33.1% and 33.6%, respectively.

The bearing capacity of Sq-NE, Sq-NE-Ns, and Sq-NE-Al columns is 719.5, 805, and 792.5 kN, respectively. The use of concrete jackets containing silica nanoparticles, waste paper sludge ash, and acrylic resin in the samples cured in normal water environment increased the bearing capacity by 11.9% and 10.1%, respectively. The bearing capacity of Sq-SE, Sq-SE-Ns, and Sq-SE-Al columns is 622, 744.5, and 747 kN, respectively. The use of concrete jackets containing silica nanoparticles, waste paper sludge ash, and acrylic resin in samples cured in sulfated water environment increased the bearing capacity by 19.7% and 20.1%, respectively (Figure 10).

3.4. Comparison of Ductility of Columns in Different States. The ductility of concrete columns is usually evaluated using the ductility index (coefficient). The load-deflection curve was used to define ductility. The ductility coefficient is obtained from the following equation [28, 49]:

$$\mu = \frac{\Delta_{0.85}}{\Delta_u}. \quad (1)$$

In this equation, $\Delta_{0.85}$ is the deflection corresponding to 85% of the maximum load, and Δ_u is the deflection corresponding to the maximum load. In Figure 11, the ductility coefficient of columns in different states is compared with

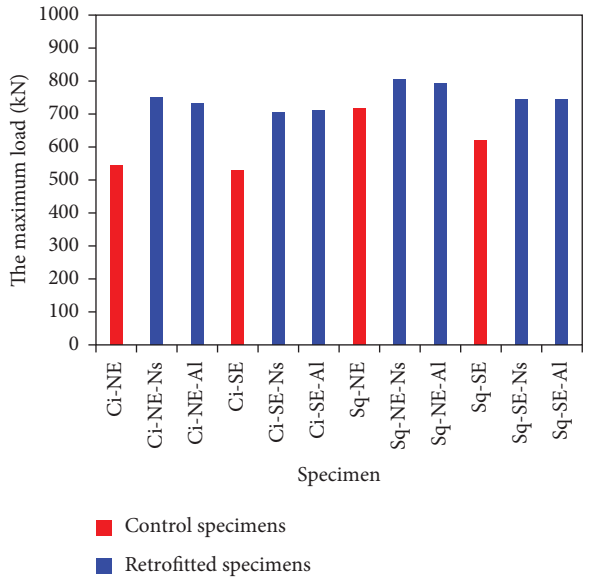

Figure 9: Comparison of the bearing capacity of columns in different states.

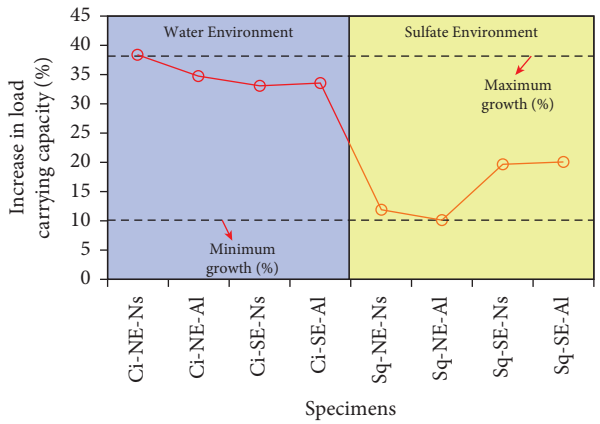

Figure 10: The percentage increase in the bearing capacity of circular and square columns retrofitted with the proposed jacket compared to the control samples.

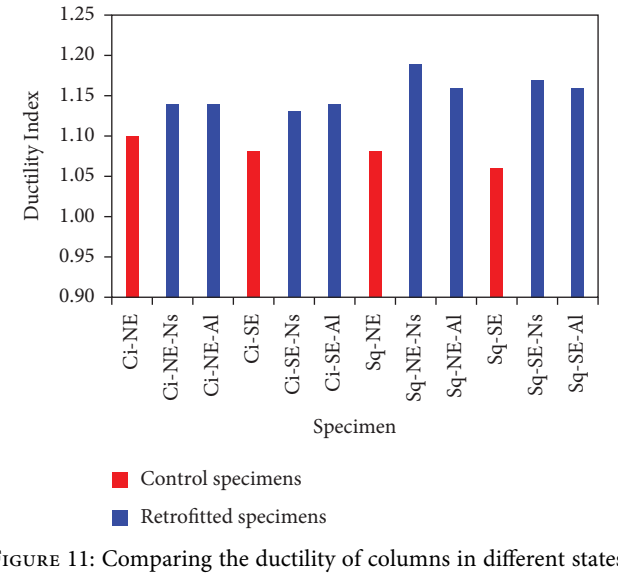

Figure 11: Comparing the ductility of columns in different states.

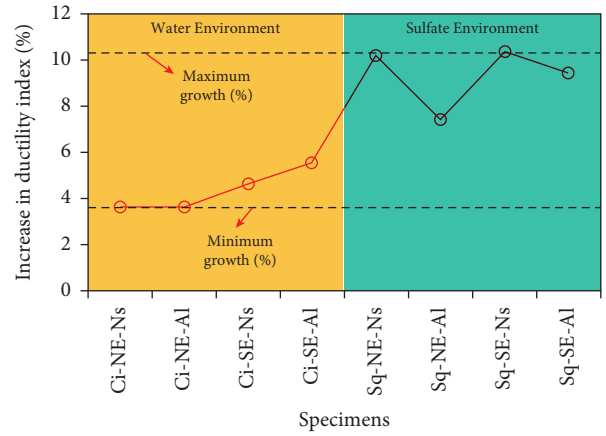

Figure 12: The increase in the ductility index of circular and square columns retrofitted with the proposed jacket compared to the control samples.

each other. Also, in Figure 12, the percentage increase in the ductility coefficient of reinforced samples compared to the control sample is presented. In all cases, the use of the proposed jacket increased the ductility coefficient of the columns.

The ductility coefficient of Ci-NE, Ci-NE-Ns, and Ci-NE-Al columns is 1.1, 1.14, and 1.14, respectively. The use of concrete jackets containing silica nanoparticles, waste paper sludge ash, and acrylic resin in samples cured in normal water environment increased the ductility by about 3%.

The ductility coefficient of Ci-SE, Ci-SE-Ns, and Ci-SE-Al columns is 1.08, 1.13, and 1.14, respectively. The use of concrete jacket containing silica nanoparticles, waste paper sludge ash, and acrylic resin in cylindrical samples cured in sulfated water environment increased the ductility coefficient by 5 and 6%, respectively.

The ductility coefficient of Sq-NE, Sq-NE-Ns, and Sq-NE-Al columns is 1.08, 1.19, and 1.16, respectively. The use of concrete jacket containing silica nanoparticles, waste paper sludge ash, and acrylic resin in samples cured in normal water environment increased the ductility coefficient by 10% and 7%, respectively. The ductility coefficient of Sq-SE, Sq-SE-Ns, and Sq-SE-Al columns is 1.06, 1.17, and 1.16, respectively. The use of concrete jacket containing silica nanoparticles, waste paper sludge ash, and acrylic resin in samples cured in sulfated water environment increased the bearing capacity by 10.4% and 9.4%, respectively. In Figure 13, the simultaneous comparison of ductility-maximum load in the investigated samples is discussed. As can be seen in all the samples where the bearing capacity has increased, the ductility has also improved. The damage in nonretrofitted columns (control samples) was sudden, and there were no significant signs to predict it. This is while in the retrofitted samples, a number of cracks were formed on

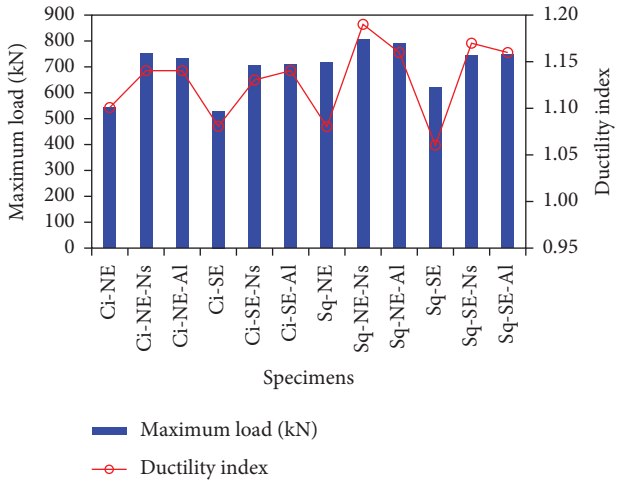

Figure 13: Simultaneous comparison of ductility-maximum load in the examined samples.

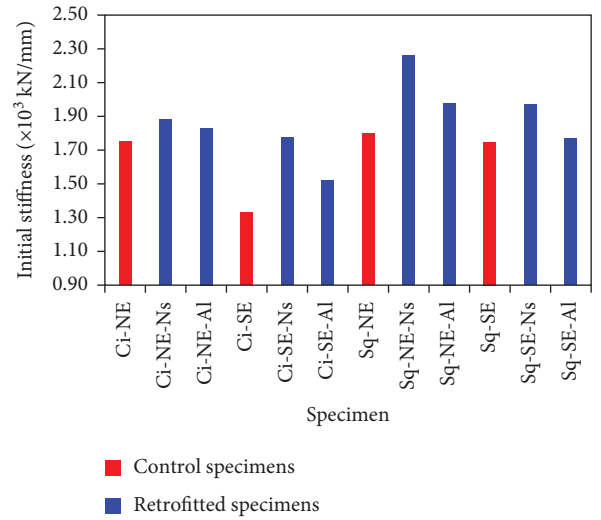

Figure 14: Comparing the stiffness of columns in different states.

the jacket surfaces at first, and after a while, the central core reached the failure point.

3.5. Comparison of the Stiffness of Columns in Different States. The stiffness of the columns is another parameter that was chosen to compare the behavior of the columns in different states. According to ACI 318M-05 [50], the stiffness of the columns is calculated from the following equation:

$$k = \frac{P_{0.45}}{\Delta_{0.45}}. \quad (2)$$

In this equation, $P_{0.45}$ is the load corresponding to 45% of the maximum load, and $\Delta_{0.45}$ is the deflection corresponding to 45% maximum load.

In Figure 14, the stiffness of columns in different states is compared. The stiffness of Ci-NE, Ci-NE-Ns, and Ci-NE-Al columns is 1.75, 1.88, and 1.83, respectively. The use of concrete jackets containing silica nanoparticles, waste paper sludge ash, and acrylic resin in the samples cured in normal water environment increased the stiffness by about 7 and 5%, respectively.

The stiffness of Ci-SE, Ci-SE-Ns, and Ci-SE-Al columns is 1.33, 1.77, and 1.52, respectively. The use of concrete jacket containing silica nanoparticles, waste paper sludge ash, and acrylic resin in cylindrical samples cured in sulfated water environment increased the stiffness by 33 and 14%, respectively. The stiffness of Sq-NE, Sq-NE-Ns, and Sq-NE-Al columns is 1.8, 2.26, and 1.98, respectively. The use of concrete jackets containing silica nanoparticles, waste paper sludge ash, and acrylic resin in the samples cured in normal water environment increased the stiffness by 26% and 10%, respectively. The stiffness of Sq-SE, Sq-SE-Ns, and Sq-SE-Al columns is 1.75, 1.97, and 1.77, respectively. The use of concrete jacket containing silica nanoparticles, waste paper sludge ash, and acrylic resin in samples treated in sulfated water environment increased the stiffness by 13% and 2%, respectively.

4. Conclusion

In this study, the combined use of waste paper sludge ash in combination with nanoparticles in concrete was investigated. A number of concrete columns were built as the column of the bridge and retrofitted using concrete jackets containing silica nanoparticles, aluminium oxide nanoparticles, waste paper waste ash, and acrylic resin. The variables in this section included the geometric shape of the column (square and circular) and the type of nanoparticles used in the coating (silica and aluminium) and the operating environment of the columns (normal and sulfated water). A summary of the most important results is presented:

(i) The positive effect of using aluminium oxide nanoparticles in improving the strength of the bridge columns confirms the results of other studies in the field of improving the mechanical characteristics of concrete. Based on previous research, aluminium oxide nanoparticles can react with calcium hydroxide resulting from cement hydration and lead to calcium silicate gel, which is an important factor in concrete strength. In this study, the combined use of aluminium oxide nanoparticles and waste paper sludge ash was also effective, and its use in the jacket led to the strengthening of the bridge column.

(ii) The combined use of aluminium oxide nanoparticles and waste paper sludge ash improved the compressive strength, tensile strength, flexural strength, and durability characteristics. These factors can increase the axial load capacity of bridge columns. The proposed concrete jacket can effectively reduce the corrosion of concrete and steel reinforcements used in it and increase the bridge's useful life.

(iii) Concrete jackets containing nanoparticles and waste paper ash increase ductility by creating external confinement in critical areas or the entire

external surfaces and make the columns able to withstand more forces. The pozzolans used in the proposed concrete jackets improved the load-bearing capacity by enhancing the durability properties.

(iv) The use of waste paper ash in combination with silica nanoparticles and aluminium oxide nanoparticles improved the porosity of concrete by reducing the large capillary pores; they have improved the concrete structure and reduced the distribution of cracks.

(v) There was no significant separation between the concrete jacket and the concrete surface of the main column. The issue of adhesion of concrete jacket to the surface of old concrete is very important. Because if there is no necessary continuity, the jacket is not very effective in bearing the load. But if the required adhesion is created, the load will increase, and the necessary continuity will be provided.

(vi) Nanosilica and aluminium oxide nanoparticles, having a high specific surface, are combined with hydrated cement and act very well in terms of adhesion and prevent the production of more calcium hydroxide crystals and fill fine cracks.

(vii) In columns with a circular cross section, the change in the curing environment has a greater effect on the number and distribution of cracks. The number and length of the cracks in the circular columns cured in the sulfated environment are many times more than those created in the circular columns cured in the normal water environment.

(viii) The use of the proposed jackets in all cases increased the load capacity from 10 to 38% depending on the processing environment and the type of nanoparticles. That is, the use of concrete jackets containing silica nanoparticles, waste paper ash, and acrylic resin in the samples processed in normal water environment has increased the bearing capacity by 38% and 34.8%, respectively.

(ix) The use of concrete jackets containing silica nanoparticles, waste paper sludge ash, and acrylic resin in cylindrical samples treated in a sulfated water environment increased the bearing capacity by 33.1% and 33.6%, respectively.

(x) The use of concrete jackets containing silica nanoparticles, waste paper sludge ash, and acrylic resin in the samples processed in a normal water environment increased the bearing capacity by 11.9% and 10.1%, respectively.

(xi) The use of concrete jackets containing silica nanoparticles, waste paper sludge ash, and acrylic resin in samples treated in a sulfated water environment increased the bearing capacity by 19.7% and 20.1%, respectively.

(xii) The ductility also improved in all samples where the load capacity increased. The damage in non-retrofitted columns (control samples) was sudden, and there were no significant signs to predict it. This is while in the retrofitted samples, a number of cracks were formed on the jacket surfaces at first, and after a while, the central core reached the failure point.

Data Availability

All data generated or analyzed during this study are included in the manuscript.

Conflicts of Interest

The authors declare that they have no conflicts of interest.

References

[1] X. Ma and H. Yang, "The important role of civilized construction-a case study of flood control measures in a bridge construction of Gansu province, China IOP Conference Series: earth and Environmental Science," *IOP Conference Series: Earth and Environmental Science*, vol. 189, no. 2, Article ID 022026, 2018.

[2] H. Qiang, J. I. A. Zhen-lei, H. E. Wei-li, X. I. A. O. Yong-ming, J. I. A. Jun-feng, and D. U. Xiu-li, "Seismic design method and its engineering application of self-centering double-column rocking bridge," *China Journal of Highway and Transport*, vol. 30, no. 12, p. 169, 2017.

[3] Y. L. Zhou, Q. Han, X. L. Du, J. Q. Zhang, S. S. Cheng, and J. Y. Chen, "Additional viscous dampers for double-column rocking bridge system: seismic response and overturning analysis," *Soil Dynamics and Earthquake Engineering*, vol. 141, Article ID 106504, 2021.

[4] S. C. Zhou, C. Demartino, J. J. Xu, and Y. Xiao, "Effectiveness of CFRP seismic-retrofit of circular RC bridge piers under vehicular lateral impact loading," *Engineering Structures*, vol. 243, Article ID 112602, 2021.

[5] D. Skokandić, A. Vlašić, M. Kušter Marić, M. Srbić, and A. Mandić Ivanković, "Seismic assessment and retrofitting of existing road bridges: state of the art review," *Materials*, vol. 15, no. 7, p. 2523, 2022.

[6] R. Zhang, R. Zhao, Z. Liu, K. Chen, P. Hu, and Z. Liu, "Cyclic behavior of existing flexure-dominated RC bridge columns retrofitted by ECC jackets in the region of plastic hinge," *Engineering Structures*, vol. 269, Article ID 114820, 2022.

[7] S. Zhuang, Q. Wang, and M. Zhang, "Water absorption behaviour of concrete: novel experimental findings and model characterization," *Journal of Building Engineering*, vol. 53, Article ID 104602, 2022.

[8] B. Bhushan Jindal, P. Jangra, and A. Garg, "Effects of ultra fine slag as mineral admixture on the compressive strength, water absorption and permeability of rice husk ash based geopolymer concrete," *Materials Today Proceedings*, vol. 32, pp. 871–877, 2020.

[9] M. B. Asil and M. M. Ranjbar, "Hybrid effect of carbon nanotubes and basalt fibers on mechanical, durability, and microstructure properties of lightweight geopolymer

concretes," *Construction and Building Materials*, vol. 357, Article ID 129352, 2022.

[10] T. Ji, "Preliminary study on the water permeability and microstructure of concrete incorporating nano-SiO2," *Cement and Concrete Research*, vol. 35, no. 10, pp. 1943–1947, 2005.

[11] M. Mao, D. Zhang, Q. Yang, and W. Zhang, "Study of durability of concrete with fly ash as fine aggregate under alternative interactions of freeze-thaw and carbonation," *Advances in Civil Engineering*, vol. 2019, Article ID 4693893, 15 pages, 2019.

[12] H. Du, H. J. Gao, and S. D. Pang, "Improvement in concrete resistance against water and chloride ingress by adding graphene nanoplatelet," *Cement and Concrete Research*, vol. 83, pp. 114–123, 2016.

[13] M. Peng and L. M. Zhang, "Analysis of human risks due to dam-break floods—part 1: a new model based on Bayesian networks," *Natural Hazards*, vol. 64, no. 1, pp. 903–933, 2012.

[14] N. I. Karpenko, V. N. Yarmakovsky, and D. Z. Kadiev, "Influence of variable stress state of concrete on its frost resistance," *InMaterials Science Forum*, vol. 945, pp. 169–175, 2019.

[15] A. S. Abdulrahman, M. Ismail, and M. S. Hussain, "Inhibiting sulphate attack on concrete by hydrophobic green plant extract," *InAdvanced Materials Research*, vol. 250, pp. 3837–3843, 2011.

[16] M. Małek, W. Łasica, M. Jackowski, and M. Kadela, "Effect of waste glass addition as a replacement for fine aggregate on properties of mortar," *Materials*, vol. 13, no. 14, p. 3189, 2020.

[17] I. A. Khalhen and R. Aghayari, "Impact resistance of concrete containing LLDPE–waste tire rubber and silica fume," *Journal of Rehabilitation in Civil Engineering*, vol. 11, no. 1, pp. 60–75, 2023.

[18] A. A. Khalil, A. Tawfik, A. A. Hegazy, and M. F. El-Shahat, "Effect of some waste additives on the physical and mechanical properties of gypsum plaster composites," *Construction and Building Materials*, vol. 68, pp. 580–586, 2014.

[19] S. Ahmad, M. I. Malik, M. B. Wani, and R. Ahmad, "Study of concrete involving use of waste paper sludge ash as partial replacement of cement," *IOSR Journal of Engineering*, vol. 3, no. 11, pp. 06–15, 2013.

[20] H. S. Wong, R. Barakat, A. Alhilali, M. Saleh, and C. R. Cheeseman, "Hydrophobic concrete using waste paper sludge ash," *Cement and Concrete Research*, vol. 70, pp. 9–20, 2015.

[21] M. A. Fauzi, H. Sulaiman, A. R. M. Ridzuan, and A. N. Azmi, "The effect of recycled aggregate concrete incorporating waste paper sludge ash as partial replacement of cement," *AIP conference proceedings*, vol. 1774, Article ID 030007, 2016, October.

[22] N. K. Bui, T. Satomi, and H. Takahashi, "Influence of industrial by-products and waste paper sludge ash on properties of recycled aggregate concrete," *Journal of Cleaner Production*, vol. 214, pp. 403–418, 2019.

[23] B. Meko and J. Ighalo, "Utilization of waste paper ash as supplementary cementitious material in C-25 concrete: evaluation of fresh and hardened properties," *Cogent Engineering*, vol. 8, no. 1, Article ID 1938366, 2021.

[24] S. S. Sharipudin and A. R. M. Ridzuan, "Influence of waste paper sludge ash (WPSA) and fine recycled concrete aggregate (FRCA) on the compressive strength characteristic of foamed concrete," *Advanced Materials Research*, vol. 626, pp. 376–380, 2013.

[25] F. Delaram, Y. Mohammadi, and M. Adlparvar, "Evaluation of the combined use of waste paper sludge ash and nanomaterials on mechanical properties and durability of high strength concretes," *International Journal of Engineering*, vol. 34, no. 7, pp. 1653–1666, 2021.

[26] J. P. Azar, M. Najarchi, B. Sanaati, M. M. Najafizadeh, and S. M. Mirhosseini, "The experimental assessment of the effect of paper waste ash and silica fume on improvement of concrete behavior," *KSCE Journal of Civil Engineering*, vol. 23, no. 10, pp. 4503–4515, 2019.

[27] M. Mavroulidou, B. Feruku, and G. Boulouki, "Properties of structural concrete with high-strength cement mixes containing waste paper sludge ash," *Journal of Material Cycles and Waste Management*, vol. 24, no. 4, pp. 1317–1332, 2022.

[28] R. Singh, M. Patel, and K. S. Sohal, "The potential use of waste paper sludge for sustainable production of concrete—a review," *Recent Advancements in Civil Engineering*, vol. 172, pp. 365–374, 2022.

[29] B. B. Mitikie and D. T. Waldtsadik, "Partial replacement of cement by waste paper pulp ash and its effect on concrete properties," *Advances in Civil Engineering*, vol. 2022, Article ID 8880196, 12 pages, 2022.

[30] Z. B. Haber, J. F. Munoz, I. De la Varga, and B. A. Graybeal, "Bond characterization of UHPC overlays for concrete bridge decks: laboratory and field testing," *Construction and Building Materials*, vol. 190, pp. 1056–1068, 2018.

[31] W. Li, H. Liang, Y. Lu, J. Xue, and Z. Liu, "Axial behavior of slender RC square columns strengthened with circular steel tube and sandwiched concrete jackets," *Engineering Structures*, vol. 179, pp. 423–437, 2019, þ.

[32] J. Xie, Q. Fu, and J. B. Yan, "Compressive behaviour of stub concrete column strengthened with ultra-high performance concrete jacket," *Construction and Building Materials*, vol. 204, pp. 643–658, 2019.

[33] A. He, J. Cai, Q. J. Chen, X. Liu, P. Huang, and X. L. Tang, "Seismic behaviour of steel-jacket retrofitted reinforced concrete columns with recycled aggregate concrete," *Construction and Building Materials*, vol. 158, pp. 624–639, 2018.

[34] J. Jia, L. Zhao, S. Wu, X. Wang, Y. Bai, and Y. Wei, "Experimental investigation on the seismic performance of low-level corroded and retrofitted reinforced concrete bridge columns with CFRP fabric," *Engineering Structures*, vol. 209, Article ID 110225, 2020.

[35] Astm C330/C330M-17a, *Standard Specification for Lightweight Aggregates for Structural Concrete*, ASTM International, West Conshohocken, PA, USA, 2017.

[36] Astm C150/C150M-20, *Standard Specification for Portland Cement*, ASTM International, West Conshohocken, PA, USA, 2020.

[37] Z. Li, H. Wang, S. He, Y. Lu, and M. Wang, "Investigations on the preparation andmechanical properties of the nano-alumina reinforced cement composite," *Materials Letters*, vol. 60, no. 3, pp. 356–359, 2006.

[38] Astm C494/C494M-19, *Standard Specification for Chemical Admixtures for Concrete*, ASTM International, West Conshohocken, PA, USA, 2019.

[39] Astm D75/D75M-14, *Standard Practice for Sampling Aggregates*, ASTM International, West Conshohocken, PA, USA, 2014.

[40] ASTM C1602/C1602M-18, *Standard Specification for Mixing Water Used in the Production of Hydraulic Cement Concrete*, ASTM International, West Conshohocken, PA, USA, 2018.

[41] Aci Committee 211.1-91, *Standard Practice for Selecting Proportions for Normal, Heavyweight and Mass Concrete*, American Concrete Institute, Farmington Hills, MI, USA, 2009.

[42] A. Faez, a. Sayari, and S. Manie, "Mechanical and rheological properties of self-compacting concrete containing Al2O3 nanoparticles and silica fume," *Iranian Journal of Science and Technology, Transactions of Civil Engineering*, vol. 44, no. 1, pp. 217–227, 2020.

[43] M. Ghanbari, O. Kohnehpooshi, and M. Tohidi, "Experimental study of the combined use of fiber and nano silica particles on the properties of lightweight self compacting concrete," *International Journal of Engineering*, vol. 33, no. 8, pp. 1499–1511, 2020.

[44] H. Heidarzad Moghaddam, A. Maleki, and M. A. Lotfollahi-Yaghin, "Durability and mechanical properties of self-compacting concretes with combined use of aluminium oxide nanoparticles and glass fiber," *International Journal of Engineering*, vol. 34, no. 1, pp. 26–38, 2021.

[45] J. Gong, L. Zhu, J. Li, and D. Shi, "Silica fume and nanosilica effects on mechanical and shrinkage properties of foam concrete for structural application," *Advances in Materials Science and Engineering*, vol. 2020, Article ID 3963089, 10 pages, 2020.

[46] C. Honglei, J. Zuquan, W. Penggang, W. Jianhong, and L. Jian, "Comprehensive resistance of fair-faced concrete suffering from sulfate attack under marine environments," *Construction and Building Materials*, vol. 277, Article ID 122312, 2021.

[47] X. Cheng, W. Tian, J. Gao, and Y. Gao, "Performance evaluation and lifetime prediction of steel slag coarse aggregate concrete under sulfate attack," *Construction and Building Materials*, vol. 344, Article ID 128203, 2022.

[48] S. Gao, J. Jin, G. Hu, and L. Qi, "Experimental investigation of the interface bond properties between SHCC and concrete under sulfate attack," *Construction and Building Materials*, vol. 217, pp. 651–663, 2019.

[49] J. B. Yan, X. T. Wang, and T. Wang, "Compressive behaviour of normal weight concrete confined by the steel face plates in SCS sandwich wall," *Construction and Building Materials*, vol. 171, pp. 437–454, 2018.

[50] Aci 318M–2005, *Building Code Requirements for Structural Concrete and Commentary*, American Concrete Institute, Farmigton Hills, MI, USA, 2005.